

Destructive-treatment-free Rapid Polymer-assisted Metal

Deposition for Versatile Electronic Textiles

Yaokang Zhang¹, Yufeng Luo¹, Lei Wang¹, Pui Fai Ng¹, Hong Hu¹, Fan Chen¹, Qiyao Huang^{1,3},
Zijian Zheng^{1,2,3,4,*}

1. Laboratory for Advanced Interfacial Materials and Devices, School of Fashion and Textiles, the Hong Kong Polytechnic University, Hong Kong, China
2. Department of Applied Biology and Chemical Technology, Faculty of Science, The Hong Kong Polytechnic University, Hong Kong SAR, China
3. Research Institute for Intelligent Wearable Systems, The Hong Kong Polytechnic University, Hong Kong SAR, China
4. Research Institute for Smart Energy, The Hong Kong Polytechnic University, Hong Kong SAR, China

E-mail: zijian.zheng@polyu.edu.hk

Keywords: polymer-assisted metal deposition, electronic textile, surface treatment, washability, wearable electronics

Abstract

Highly conductive, durable, and breathable metal-coated textiles are critical building block materials for future wearable electronics. In order to enhance the metal adhesion on the textile surface, existing solution-based approaches to preparing these materials require time-consuming pre-synthesis and/or pre-modification processes, typically in the order of tens of minutes to hours, on textiles prior to metal plating. Herein, we report an UV-induced rapid polymer-assisted metal deposition (r-PAMD) that offers a destructive-treatment-free process to deposit highly conductive metals on a wide variety of textile materials, including cotton, polyester, nylon, Kevlar, glass fiber, and carbon cloth. In comparison to the state of the arts, r-PAMD significantly shortens the modification time to several minutes, and is compatible with the roll-to-roll fabrication manner. Moreover, the deposited metals show outstanding adhesion, which withstands rigorous flexing, abrasion and machine washing tests. We demonstrate that these metal-coated textiles are suitable for applications in two vastly different fields, being wearable and washable sensors, and lithium batteries.

Introduction

Electronic textiles (E-textiles), which enable sensors,^{1, 2} photovoltaics,³ supercapacitors,^{4, 5} nanogenerators,⁶ and batteries^{7, 8} in wearable textile materials, are indispensable for future wearable electronics. The development of such E-textile requires scalable production of lightweight, highly conductive, and flexible conducting textiles.⁹⁻¹³ Among them, metal-coated fabrics, which are lightweight, soft, and skin-compatible, show great potential for wearable energy harvesting, energy storage, and health monitoring devices. However, traditional vacuum deposition technologies for metal coating suffer from poor adhesion and incomplete coating of the materials due to the three-dimensional structures of the textile substrates.^{14, 15} In addition, depositing metals on textile materials via vacuum technologies is not cost efficient in terms of material utilization and throughput.¹⁶ As a result, recent researches focus on solution-based technologies to depositing metals on textiles.^{17, 18} Such solution processes are highly compatible with high throughput and scalable roll-to-roll (R2R) process, which is widely accepted by the textile industry.^{19, 20}

The most commonly used solution-based technologies to producing metal-coated textiles is autocatalytic electroless deposition (ELD).^{21, 22} Such process requires activation of substrates with catalytic moieties such as Pd and Ag salts, which can facilitate the *in situ* reduction of metals in the plating bath.²³⁻²⁶ However, direct electroless deposition on textile materials often suffers from wetting and adhesion issues, because of the poor interaction between catalysts and the textile surfaces especially for those hydrophobic ones.^{24, 27} To address this issue, both physical and chemical pretreatments are adopted prior to the metal deposition. Physical pretreatment includes

plasma treatment,²⁸ laser etching,²⁹ and high-energy UV irradiation.³⁰ Chemical pretreatments such as NaOH mercerization,³¹ acid activation,³² and self-assembled monolayer (SAM) modification³³ have also been developed to improve the adhesion of catalysts. Recently, a mild chemical modification technology namely polymer-assisted deposition (PAMD) was reported.^{15, 34-37} In such process, functional polymers possessing a high affinity to the catalytic moieties are chemically grafted on target substrates. The functional polymers serve as anchors between the catalytic moieties and the substrates to address the wetting issue of catalytic moieties on the substrates. Such polymer modification process is more gentle than conventional harsh pretreatment processes, and is applicable to many conventional textile materials, such as yarns and fabrics made of cotton, polyester, Kevlar, and spandex.³⁸⁻⁴¹ However, these pretreatments are time-consuming and often show poor versatility of applicable textile materials.^{32, 42, 43} In addition, many of them weaken the strength of the textiles, which significantly limits the practical applications.⁴⁴⁻⁴⁶

Herein, we report a destructive-treatment-free and pre-synthesis-free rapid PAMD (r-PAMD) approach based on UV-induced *in situ* crosslinking of functional precursors on textile surfaces. In comparison to the literature, the entire polymer modification and catalyst activation process is significantly shortened from tens of minutes or even hours to 3 min (**Table 1**). We demonstrate fast deposition of Ni, Cu, Ag, and Au on a wide variety of textile materials including cotton, polyester, nylon, Kevlar, carbon, and glass fiber, regardless of their textile structures. Very importantly, r-PAMD causes no damage to the strength of textile materials, while still maintaining outstanding adhesion of the metal. These E-textiles survive from harsh washing and abrasion tests, showing insignificant degradation of electrical conductivity. We demonstrate the applications of these E-textiles for wearable electrocardiogram (ECG) and strain sensors that can withstand 50

machine washes. Furthermore, we show that the as-made composite Au-Cu coated cotton fabrics can be employed as lithiophilic current collectors for Li metal batteries.

Table 1. Comparison of representative electroless metal deposition technologies reported in literature

Textile Material(s)	Modification Method	Destructive-treatment Required	Pre-synthesis Required/ Duration	Duration of Modification and Activation	Applicable Metal(s)	Refs.
polyester	colloid catalyst coating	No	Yes/> 3 h	11 min	Cu	47
polyester, nylon	laser scribing	Yes	No	> 10 min	Ni	48
nylon 6,6	supercritical CO ₂	No	No	20~120 min	Ni	49
cotton, filter paper	SnCl ₄ ²⁻ sensitization	No	No	15 min	Ni, Co, Cu, Ag	50
core-spun elastic yarns	curcumin coating	No	No	45 min	Cu, Ni	51
polyethylene	polydopamine coating	No	No	2 h	Ag, Cu, Ni	52
cotton, filter paper, weighing paper	crosslinking of photoreactive copolymer	No	Yes/> 24 h	25 min	Cu, Ni, Ag	53
cotton, polyester, nylon, Kevlar, carbon fiber, glass fiber	UV-induced <i>in situ</i> crosslinking	No	No	3 min	Ni, Cu, Ag, Au	This work

Materials and Methods

Materials

Kevlar yarns and knitted Kevlar fabrics were purchased from Tansoz High Performance Rope & Webbing Co., Ltd. Carbon cloths were purchased from Taiwan CeTech Co. Ltd. Copper (II) sulfate pentahydrate ($\text{CuSO}_4 \cdot 5\text{H}_2\text{O}$), silver nitrate (AgNO_3), and nickel (II) sulfate hexahydrate ($\text{NiSO}_4 \cdot 6\text{H}_2\text{O}$) were purchased from UNI-CHEM. Potassium sodium tartrate tetrahydrate ($\text{KNaC}_4\text{H}_4\text{O}_6 \cdot 4\text{H}_2\text{O}$) and sodium hydroxide (NaOH) were purchased from VWR chemicals. Lactic acid was purchased from Acros organics. Ammonia solution ($\text{NH}_3 \cdot \text{H}_2\text{O}$) was purchased from International Laboratory USA. ammonium tetrachloropalladate (II) ($(\text{NH}_4)_2\text{PdCl}_4$) was purchased from Alfa Aesar. All other chemicals were purchased from Sigma-Aldrich.

Polymer Modification and Catalyst Activation

The textiles were cleaned in ultrasonification baths of acetone, isopropanol, and water for 15 min, respectively. Then, the textiles were dipped in an ethanol solution of 2.0 g L^{-1} 2,2-bimethoxy-2-phenylacetophenone (DMPA), 16.0 g L^{-1} *N,N'*-Methylenebisacrylamide (NMBA), and 30.0 mL L^{-1} [2-(methacryloyloxy)ethyl] trimethylammonium chloride (METAC, 75% in water) for 1 min. Afterwards, the textiles were cured under an UV lamp ($\text{UVA } 80.0 \text{ mW cm}^{-2}$) for 1 min, and then rinsed with water for another 1 min. Finally, the polymer modified textiles were immersed in 3.2 g L^{-1} $(\text{NH}_4)_2\text{PdCl}_4$ for 1 min, followed by rinsing with water for 1 min. For the control samples fabricated via conventional PAMD technology, a silanization and free-radical polymerization approach was adopted.³⁹

Electroless Deposition of Metals

The electroless plating bath of Cu was a 1:1 mixture of solution A and solution B. Solution A consisted of 52 g L⁻¹ CuSO₄·5H₂O, 48 g L⁻¹ NaOH, and 117 g L⁻¹ KNaC₄H₄O₆·4H₂O. Solution B was a diluted solution of 37% formaldehyde in water (9.5 mL L⁻¹). The catalyst activated textiles were immersed in the plating bath for 30 ~ 120 min to obtain the Cu-coated textiles. All the Cu-coated textiles for wash and abrasion tests were plated for 120 min under the same condition. The electroless plating bath of Ni was a mixture of 40 g L⁻¹ NiSO₄·6H₂O, 10 g L⁻¹ lactic acid, 20 g L⁻¹ sodium citrate, and 2 g L⁻¹ dimethylamine borane (DMAB). The solution was adjusted to pH = 8.5 with NH₃·H₂O prior to the electroless plating process, which also took 30 to 120 min. The electroless plating bath of Ag consisted of 1 g L⁻¹ Ag[NH₃]₂NO₃ and 9.5 mL L⁻¹ formaldehyde. To deposit Au on textiles electrolessly, a solution of 3.9 g L⁻¹ HAuCl₄·3H₂O, 0.4 g L⁻¹ NaOH, 7.0 g L⁻¹ NH₂OH·HCl, 11 g L⁻¹ Na₂HPO₄, 16 g L⁻¹ Na₂S₂O₃·5H₂O, and 40 g/L Na₂SO₃ was prepared, and the reaction temperature was 65 °C.

Au@Cotton Electrodes for ECG Sensing

The Au-coated cotton electrodes were obtained via electro-deposition of Au on Cu-coated cotton fabrics. The Cu-coated cotton fabrics were fabricated via the electroless deposition method mentioned above. The Au electro-deposition bath was purchased from Caswell Inc. (Caswell Plug N' Plate Kits). The electro-deposition condition was DC 4.5 V (supplied by Keithley 2400 sourcemeter) for 30 min. The Au-coated cotton fabrics were cut into circular pieces with a diameter of 2 cm, and then embroidered on a stretchable t-shirt with Ag yarns. For ECG sensing, the

electrodes or the gel patch control electrodes were connected to a portable ECG sensor (Healthforce PC-80B) with a 3-wire lead placement.

Galvanic Displacement of Au on Cu for Li Metal Batteries

The Au-Cu current collectors were obtained via galvanic displacement of Au on Cu-coated cotton fabrics, which were fabricated via the electroless deposition of Cu on cotton. The Cu-coated cotton fabrics were immersed in a 2.5 mM solution of HAuCl_4 for 1 min, and then rinsed with water. After drying with compressed air, the Au-Cu fabrics were annealed at 150 °C on a hotplate in an Ar-filled glove box for 20 min.

Electrochemical Tests

R2032-type coin batteries were assembled using the fabricated fabrics as the working electrode and lithium foil as the counter electrode in an argon-filled glove box, and one layer of Celgard 2325 was used as the separator. The electrolyte was prepared by magnetically stirring 1 M bis-trifluoromethane sulfonamide lithium (LiTFSI) and 0.2 M lithium nitrate (LiNO_3) in dioxolane (DOL) and dimethyl ether (DME) with a volume ratio of DOL: DME at 1:1. The $\text{Li}||\text{Cu}$ and $\text{Li}||\text{Au-Cu}$ half-cell was tested at a current density of 1mA cm^{-2} in the range of 0 ~ 1 V.

Material Characterization

The SEM and EDX mapping images were taken with a Tescan VEGA3 scanning electron microscope. For the cross-sectional metal-coated textile images, the samples were covered with

epoxy and polished with abrasive papers prior to the characterization. The XRD patterns were characterized with an X-ray diffractometer (Rigaku SmartLab). The XPS analysis was carried out with a Thermo Scientific Nexsa X-ray photoelectron spectrometer. Optical microscopic images were recorded with a Nikon Eclipse 80i optical microscope, and the photographs were taken with a Nikon Z 7 mirrorless camera. AATCC 135 test standard was applied to the metal-coated textiles for the wash test. The samples were washed with 1.8 kg loading in a Whirlpool WTW4955H washer. The Martindale abrasion test was carried out with an SDL Atlas M235 abrasion and pilling tester with 9 kPa weights. The abrasion test was operated under the ASTM D4966 standard. The stress-strain curves of the polyester fabrics were measured with the Instron 5566 universal testing system. The samples were prepared and tested according to the ASTM D5034-09(2013) standard.

Results and Discussion

r-PAMD for Metal-coated Textiles

Schematical illustration of the r-PAMD process is shown in **Figure 1**. Commercially available textile fabrics were dipped in an ethanol solution of UV-curable precursors, followed by a fast UV irradiation step to crosslink the catalyst-affinitive polymer on the surface of the fibers (see Experimental Section for details). The solution contained a mixture of photo-initiator 2,2-dimethoxy-2-phenylacetophenone (DMPA), crosslinker *N,N'*-methylenebisacrylamide (NMBA), and the catalyst-anchoring monomer [2-(methacryloyloxy)ethyl]trimethylammonium chloride (METAC). The UV irradiation induces the photolysis of DMPA to benzoyl radicals, which initiate the polymerization of NMBA and METAC. **As illustrated in Figure 1, textile fibers were wrapped in the crosslinked functional polymer after the UV crosslinking process. The crosslinks increase**

the strength of functional polymer coating on textile fibers, providing sufficient wear resistance against washing and abrasion. Meanwhile, METAC segments in the functional polymer show a very high affinity to PdCl_4^{2-} catalytic moieties, which originates from the strong electrostatic interaction between quaternary ammonium groups and PdCl_4^{2-} ions. After loading of the PdCl_4^{2-} moieties via ion exchange, the textiles were immersed in metal plating baths to obtain metal-coated textiles.

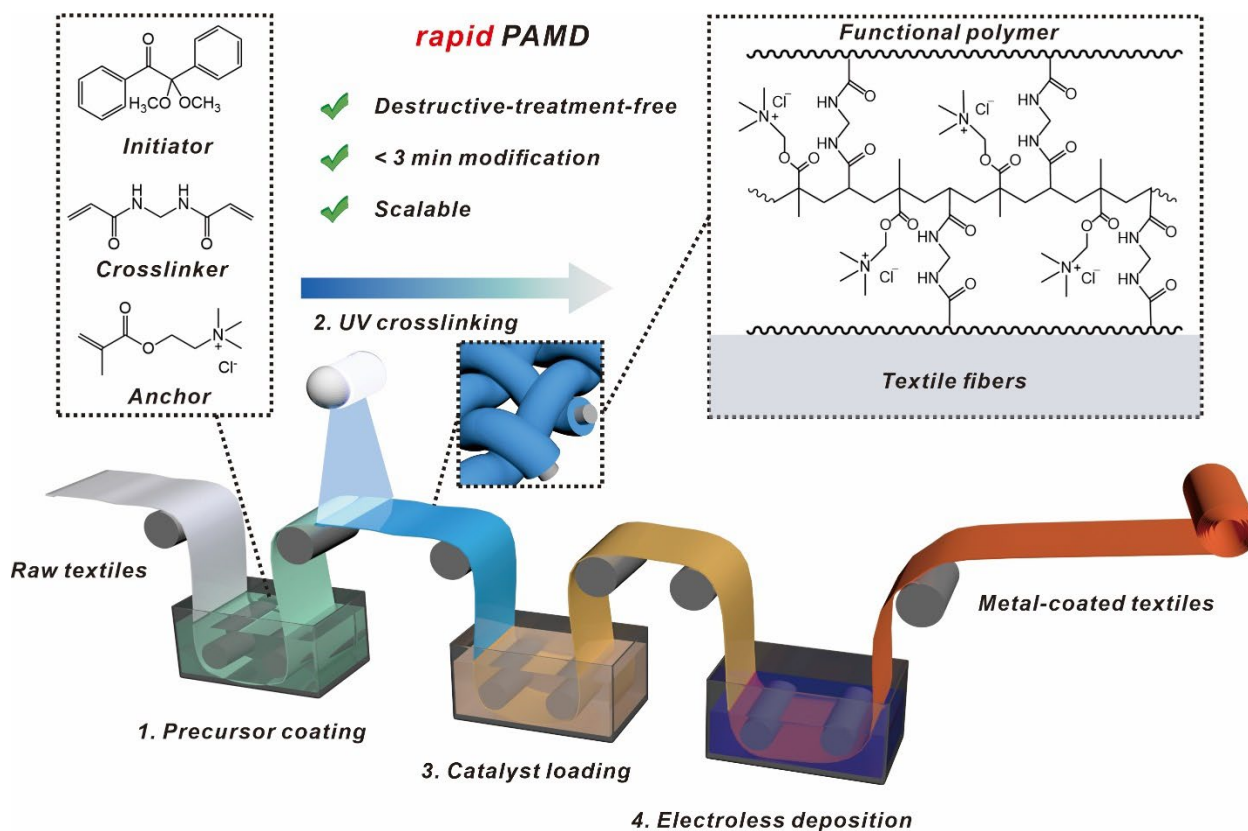


Figure 1. Scheme of the rapid polymer-assisted metal deposition (r-PAMD) process for metal deposition on textile materials.

Characterization of Metal-coated Textiles

The UV-induced *in situ* crosslinking process was investigated by Fourier-transform infrared spectroscopy (FTIR). The precursor mixture became a thermoset plastic after the UV curing process. As shown in Figure S1, the IR spectrum of precursor mixture shows absorption peaks at 1716 and 1654 cm^{-1} , referring to the C=O stretching vibration of METAC and NMBA, respectively. The peak at 1626 cm^{-1} refers to the C=C stretching vibration, which also exists in METAC and NMBA. After the UV irradiation process, the peak at 1626 cm^{-1} disappeared, which indicates the successful polymerization of METAC and NMBA. Meanwhile, the peak at 1716 cm^{-1} shifted to 1723 cm^{-1} , because the α,β -unsaturated ester was converted to saturated ester. Similar situation occurred on NMBA, which resulted in a peak shift from 1654 cm^{-1} to 1646 cm^{-1} .

The precursor solution showed good wettability to either hydrophilic cotton fabrics, or hydrophobic fabrics such as carbon cloth, glass fiber fabrics, nylon fabric, and Kevlar fabrics. To demonstrate viability of modifying the polymer on fabrics, the chemically inert and hydrophobic raw carbon cloth is used as an example (Figure S2). Before the contact angle test, both the raw carbon cloth and the modified carbon cloth were cleaned in an ultrasonification bath of ethanol for 15 min and dried at 80 °C for 10 min. The raw carbon cloth showed a high contact angle of $135.5 \pm 5.8^\circ$. In contrast, the contact angle of modified carbon cloth reduced significantly to $72.8 \pm 11.0^\circ$ at the fifth second after the contact, and became complete wetting within 10 s. This is because the METAC segment is a quaternary ammonium salt which shows a high hydrophilicity.⁵⁴

One key advantage of the UV-induced *in situ* crosslinking of r-PAMD is the absence of destructive pretreatment processes. Compared a conventional polymer modification process on NaOH-treated polyester fabrics,⁵⁵ the polyester fabrics modified via UV-induced *in situ* crosslinking showed an almost identical tensile strength to that of the raw polyester fabrics (**Figure 2A**). Another advantage of the r-PAMD process is the high adhesion provided by the crosslinked functional polymer. To study the adhesion of metals for wearable applications, we studied resistance change of Cu-coated textiles during repeated standard wash and abrasion tests. Figure 2B and C are the sheet resistance versus wash cycles of Cu-coated textiles fabricated via conventional PAMD and r-PAMD, respectively. On the one hand, the sheet resistance of Cu-coated cotton (Cu@cotton) and polyester (Cu@polyester) fabrics were very stable during 25 cycles wash test despite of the metal deposition method. On the other hand, the r-PAMD method outperformed conventional PAMD on Kevlar and nylon fabrics, which are more hydrophobic and chemically inert than cotton and polyester fabrics. The insets of Figure 2B and C are the optical images of Cu-coated nylon (Cu@nylon) textiles fabricated via both methods after 25 cycles of wash test. The Cu coating of the r-PAMD sample remained intact even after 25 cycles of washing, whereas notable peeling-off can be observed on Cu@nylon fabricated via conventional PAMD method. The abrasion test was also carried out to study the abrasion resistance of Cu-coated textiles. As shown in Figure 2D, the sheet resistance of Cu@cotton fabricated via conventional PAMD raised slightly from $\sim 0.2 \Omega \text{ sq}^{-1}$ to $\sim 1 \Omega \text{ sq}^{-1}$, while the sheet resistance of Cu@polyester increased to $> 2 \Omega \text{ sq}^{-1}$ after 2,000 cycles of abrasion. However, the sheet resistance of Cu-coated, Kevlar (Cu@Kevlar) and Cu@nylon increased significantly after 1,000 cycles of abrasion. In contrast, Cu@cotton, Cu@polyester, and Cu@Kevlar obtained via r-PAMD showed a very good stability after 2,000 cycles of abrasion: the sheet resistance of Cu@polyester and Cu@Kevlar were still $< 0.1 \Omega \text{ sq}^{-1}$,

and the sheet resistance of Cu@cotton only increased slightly to $< 0.6 \Omega \text{ sq}^{-1}$ (Figure 2E). The wash and abrasion test results are clear evidence for the high durability of r-PAMD metal layers on textile materials, especially on those inert and hydrophobic ones.

The fast and simple r-PAMD technology is beneficial for large scale fabrication of metal-coated textiles. The photograph in Figure 2F shows a roll of 18×65 cm Cu-coated cotton fabric prepared via our approach, which retained the softness of the raw cotton fabrics. We also demonstrate the successful deposition of Ni, Cu, Ag, and Au on multiple textile materials such as carbon cloth (CC), glass fiber (GF), Kevlar, and cotton via the r-PAMD technology (Figure 2G). To study the interface between textiles and metals, SEM cross-sectional images and corresponding EDX mapping images of metal-coated textiles are shown in Figure 2H. Ni, Cu, Ag, and Au coatings with a thickness ranging from ~ 1 to $4 \mu\text{m}$ were obtained via r-PAMD on Kevlar, cotton, nylon, and polyester fabrics, respectively. The metals covered the individual fibers uniformly on loose fabrics such as the knitted Kevlar and woven cotton, while the thick and continuous metal coating appeared on the outer fibers for tight textiles such as the woven nylon and polyester. Fortunately, the metals showed a good uniformity and coverage on the surface of these fabrics (Figure S3), which ensured a good conductivity of the metal-coated textiles.

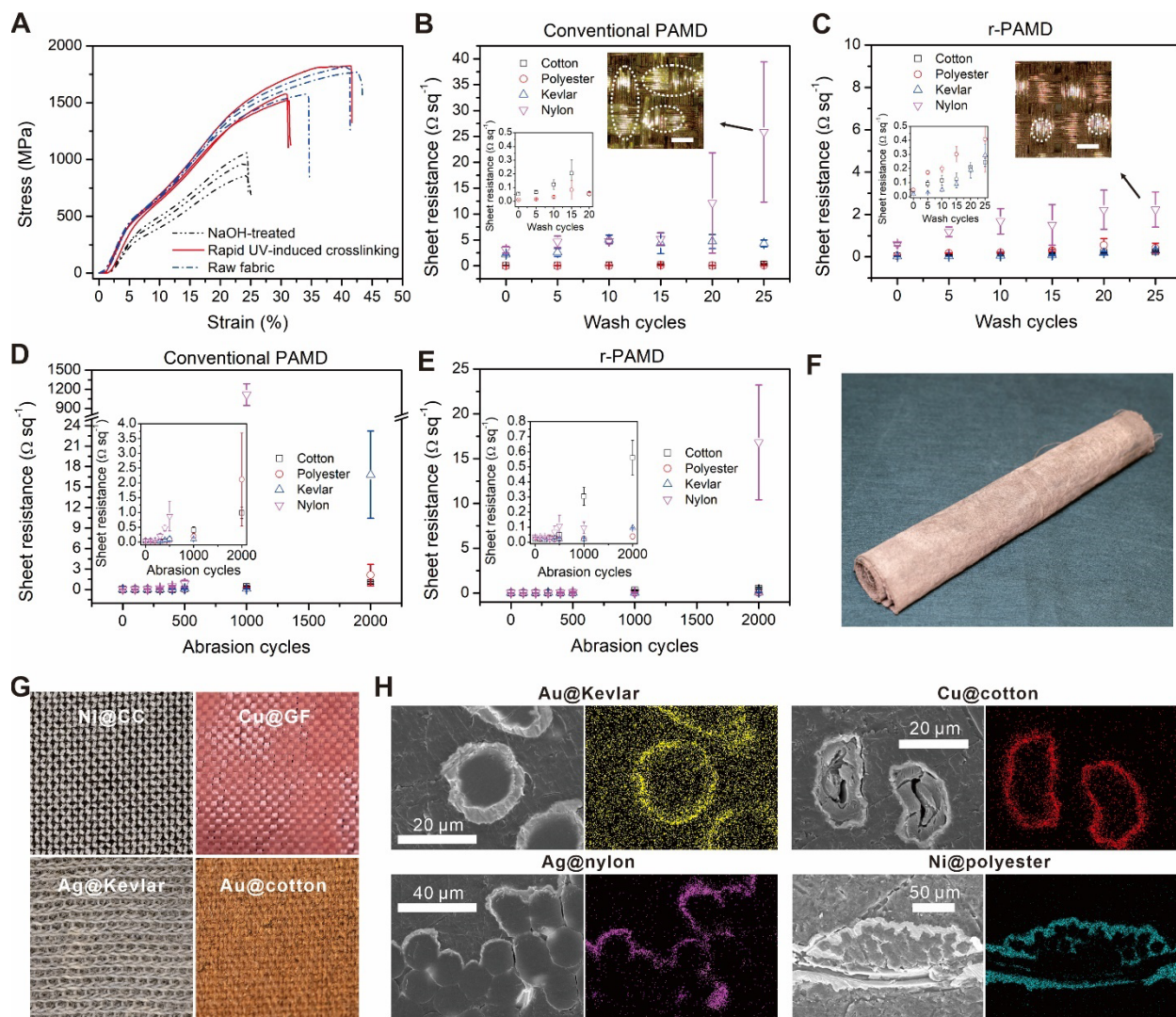


Figure 2. Characterization of metal-coated textiles. (A) Stress-strain curves of raw polyester fabrics (raw fabric), and polymer modified polyester fabrics via conventional PAMD (NaOH-treated) and r-PAMD (rapid UV-induced crosslinking). (B) and (C) Sheet resistance of Cu-coated textiles fabricated via conventional PAMD and r-PAMD during wash test (Enlarged plots are shown in insets). The wash test was carried out under AATCC 135 standard. Inset photographs are optical microscopic images of Cu@nylon samples after 25 cycles of washing. Dashed circles indicate the Cu peel-off areas. (D) and (E) Sheet resistance of Cu-coated textiles fabricated via conventional PAMD and r-PAMD during Martindale abrasion test. Enlarged plots are shown in

insets. The abrasion test was carried out under ASTM D4966 standard. (F) Photograph of a roll of 18×65 cm Cu-coated cotton fabric. (G) Photographs of Ni-coated carbon cloth (Ni@CC), Cu-coated glass fiber fabric (Cu@GF), Ag-coated Kevlar fabric (Ag@Kevlar), and Au-coated cotton fabric (Au@cotton). (H) Cross-sectional SEM images and EDX mapping of Au@Kevlar, Cu@cotton, Ag@nylon, and Ni@polyester. Yellow, red, magenta, and cyan refer to Au, Cu, Ag, and Ni, respectively.

Metal-coated Textiles for Strain and ECG Sensing

The deposition of metals could enhance the mechanical strength of yarns and fabrics. Figure S4A shows a photograph of Cu deposited on Kevlar yarns. The metal was coated uniformly even on single short fibers (Figure S4A inset). The raw Kevlar yarn showed a high Young's modulus of 2.4 GPa, which further boosted to 4.6 GPa after coating with Cu (Figure S4B). The feature of high robustness of metal-coated Kevlar yarns enables high strength and lightweight wearable conductors. For example, the Cu-coated Kevlar knitted fabrics showed a very good stability in electrical conductivity during repeated stretch and compress at a strain of 40% (Figure S5). The resistance increased gradually during the first 2,000 cycles as the fabric became loose, and then maintained stable ever since. Note that the resistance of the fabric was lower when stretched, because the tightening of the **loop knitting structure** improved the contact between each individual yarn. As a proof of concept, we demonstrate the application of the Cu-coated Kevlar knitted fabrics as strain sensors. **Figure 3A** shows the relative resistance change of the knitted fabric during cyclic stretch and compress at 10% strain with different frequencies. The fabric showed $\sim 70\%$ change in resistance at 10% strain regardless of the stretch-compress frequencies. The quasi-linear and minor hysteresis behavior (Figure 3B) of resistance change versus strain enabled the great potential

of the knitted Cu-coated Kevlar fabric for strain sensing. Figure 3C shows the resistance change of the fabric according to stepwisely increased strain. The resistance decreased $\sim 1 \Omega$ after every 2% increased strain from 0 to 8%, but the change reduced to $\sim 0.5 \Omega$ when the strain increased from 8% to 10%. The result was consistent with the $\Delta R/R_0$ -strain curves in Figure 3B.

Importantly, multilayer metal coating can be realized on the conductive textiles via additional electrodeposition (ED) or galvanic displacement (GD) after the ELD process. Figure S6 shows a piece of cotton fabric coated with ELD Cu and ~ 5 to $7 \mu\text{m}$ -thick ED Au. The ED Au-coated cotton fabrics showed a very good water vapor permeability, which was almost identical to that of raw cotton fabrics (Figure 3D). As a result, such Au-coated cotton fabrics are very promising for wearable health monitoring devices without causing allergy or discomfort. Hence, we demonstrated the application of the ED Au-coated cotton fabrics for ECG monitoring. Figure 3E shows the front view and inside-out photographs of a stretchable ECG sensing t-shirt with the ED Au-coated cotton electrodes, which showed very similar appearance and comfortability to those of an ordinary t-shirt.

More importantly, the ECG sensing t-shirt is washable (Figure 3F) thanks to the high adhesion between the metal and the textile material. We further tested the durability of the Au-coated cotton electrodes during repeated wash and abrasion tests. Figure 3G and H shows the sheet resistance of the Au-coated cotton fabrics during 50 cycles of repeated washing tests and 2,000 cycles of abrasion tests, respectively. The sheet resistance of the conductive fabric increased gradually from $26.7 \pm 3.5 \text{ m}\Omega \text{ sq}^{-1}$ to $96.3 \pm 13.1 \text{ m}\Omega \text{ sq}^{-1}$ after 50 cycles of washing. Such variation in sheet

resistance is negligible for ECG sensing. In the abrasion test, the sheet resistance of the Au-coated cotton electrodes increased from $22.2 \pm 2.3 \text{ m}\Omega \text{ sq}^{-1}$ to $643 \pm 281 \text{ m}\Omega \text{ sq}^{-1}$. As shown in Figure 3I, the performance of the t-shirt with Au-coated cotton electrodes (Au-initial) was almost identical to that of commercial disposable gel skin patches (gel patch control) for ECG sensing. More importantly, the performance of the Au-coated cotton electrodes was very stable during 50 cycles of washing (Au-initial to Au-50 wash cycles). In contrast, the commercial gel patch electrodes were out of function within 10 wash cycles due to the running-off of the gel electrolyte.

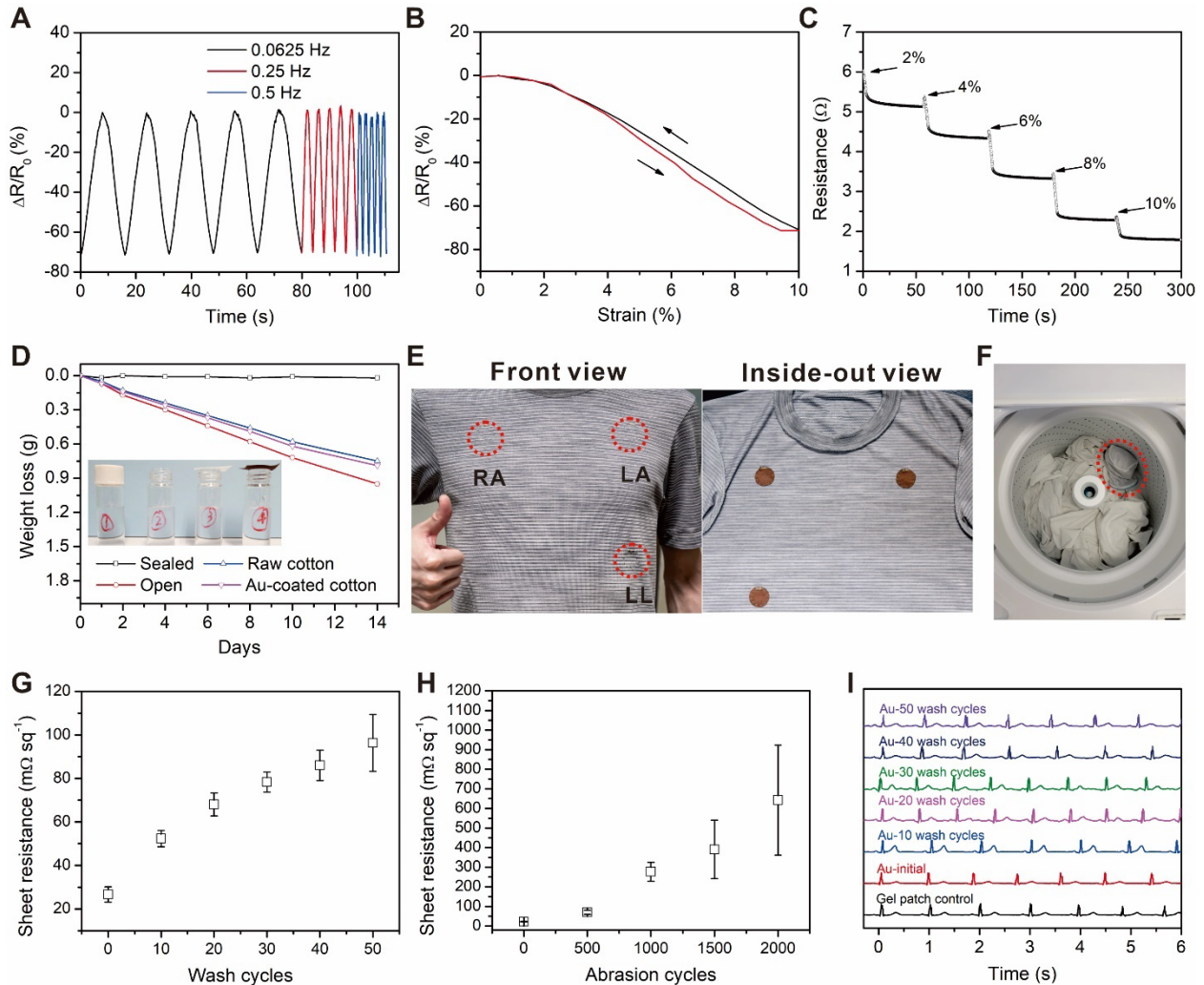


Figure 3. Metal-coated textiles for strain and ECG sensing. (A) $\Delta R/R_0$ of the Cu-coated knitted Kevlar fabric during 10% stretch-compress test at 0.0625, 0.25, and 0.5 Hz. (B) Hysteresis of the $\Delta R/R_0$ during one stretch-compress cycle at 0.25 Hz. (C) The resistance change of the Cu-coated knitted Kevlar fabric under stepwise increased strain (2% each step). e) (D) The weight loss of water in bottles sealed with cap, opened, sealed with raw cotton fabric, and sealed with Au-coated cotton fabric, respectively. Inset is a photograph of the samples. (E) Photographs of a stretchable t-shirt embroidered with Au-coated cotton electrodes for ECG sensing via a 3-lead method. (F) Photograph of the ECG sensing t-shirt (in the laundry bag labeled with red dashed circle) in a washer with 1.8 kg loading for the wash durability test. (G) and (H) The sheet resistance of Au-coated cotton fabrics during repeated washing test and Martindale abrasion test, respectively. (I) ECG signals tested with the Au-coated cotton fabric electrodes after every 10 wash cycles. Gel path control refers to the ECG signals tested with commercial gel patch electrodes.

Metal-coated Textiles for Li Metal Batteries

The high interaction energy between Au and Li reduces the overpotential for Li nucleation, and thus results in a high uniformity of Li film plated on Au surface.⁵⁶ However, direct using of expensive Au current collectors would make the cost of Li batteries unacceptable. To overcome this issue, GD can be employed to decorating Cu-coated current collectors with Au. In addition, the GD reaction generates copper oxides, which could further improve the wetting of Li, as revealed by a recent research of our group.⁵⁷ Here, proof-of-concept Au-decorated Cu@ cotton (Au-Cu@cotton) current collectors for Li metal batteries were obtained via GD reaction between HAuCl_4 and Cu-coated cotton fabrics. One additional post-annealing process, which facilitates the

diffusion of Au into the underlying Cu layer,⁵⁸ was also adopted to increase the depth of Au-Li alloys in the Cu current collector.

The high-resolution scanning electron microscopy (SEM) images (Figure S7) revealed the needle-like nanocrystals on the surface of metals. The size of the nanocrystals showed no significant change after the GD and further thermal annealing process. The generation of Cu₂O after the GD process was confirmed by the X-ray diffraction (XRD) patterns (Figure 4A). Figure S8 shows the X-ray photoelectron spectroscopy (XPS) survey of Cu, Au-Cu, and annealed Au-Cu coated cotton fabrics. The signals of Au 4*f* and Au 4*d* were observed from Au-Cu and annealed Au-Cu samples, indicating the successful decorating of Au after the GD process. The Cu 2*p* XPS spectra of as-prepared Au-Cu and annealed Au-Cu (Figure 4B and C) were compared to study the change in Cu oxidation stage before and after the annealing process. The Cu²⁺ was partially reduced after the thermal annealing, as indicated by the decrease in ratios of Cu²⁺ (~934.5 eV) and satellites (~940 to 945 eV) to Cu and Cu⁺ at ~933 eV. This result is consistent with previous reports on thermal annealing of partially oxidized Cu films.⁵⁹ Meanwhile, the thermal annealing process reduced the signals of Au 4*f* to ~½ of its original value after annealing, indicating the thermal induced diffusion of Au from surface to underlying Cu (Figure S9). The diffusion process increased the depth of Au and Au-Li alloys in the Cu current collector, which could further enhance the energy storage performance of Li metal batteries.⁶⁰

The structure of the coin cells with Au-Cu@cotton current collectors is illustrated in Figure 4D. The morphologies of the electro-deposited Li on the current collectors were characterized with

SEM to study the wetting of Li on the current collectors. Figure 4E and f show SEM images of Li-plated Cu@cotton and Au-Cu@cotton current collectors, respectively. After 10 h electrochemical deposition, the Li on the Cu current collector showed a poor coverage and a mossy morphology (red dashed circle area). The cross-sectional image reveals the accumulation of > 100 μm -thick Li on the top surface of Cu@cotton current collector, indicating a poor affinity of Li render promiscuous nucleation on the current collector. Fortunately, the decoration of Au on the current collector improved the affinity of Li on the current collectors significantly. The coverage and uniformity of Li on Au-Cu@cotton were notably higher than those of Li on Cu@cotton (Figure 4F). As shown in the cross-sectional image, the Li was spatially distributed in the entire current collector thanks to the good affinity to Au-Cu@cotton. The good affinity of Li to the Au-Cu@cotton can also be supported by its low plating overpotential. To study this, we demonstrated the charge-discharge curves of a control coin cell with Cu@cotton current collector and a coin cell with Au-Cu@cotton current collector. The coin cells went through 2 charge-discharge cycles as an activation process. As shown in Figure 4G and H, the coin cell with Au-Cu@cotton current collector showed a much smaller overpotential of 15 mV than that of the control device with Cu current collector (27 mV) at the 3rd cycle. The overpotentials of coin celled based on both Cu@cotton and Au-Cu@cotton current collectors became smaller in the following cycles, stabilized at 19 mV and 14 mV after 20th cycle, respectively. It is worth noting that the potential hysteresis of Au-Cu current collector-based devices (~ 30 mV) was also lower than that of Cu current collector-based devices (~ 40 mV), which indicates a good interface between Au-Cu@cotton current collector and Li. To show the electrochemical performance of the Au-Cu@cotton current collector, the coulombic efficiency (CE) of the coin cell with Au-Cu@cotton current collector was demonstrated in Figure 4I. The CE of the coin cells were tested in a partial

capacity of 2 mAh cm^{-2} at a current density of 1 mA cm^{-2} . The CE of the control device with Cu@cotton current collector was stable for the initial 30 cycles, and then decreased rapidly to 80% after 80 cycles. In contrast, the coin cell with Au-Cu@cotton current collector showed a significantly higher retention of $> 96.5\%$ after 80 cycles, indicating a very good stability of the Au-Cu@cotton current collector.

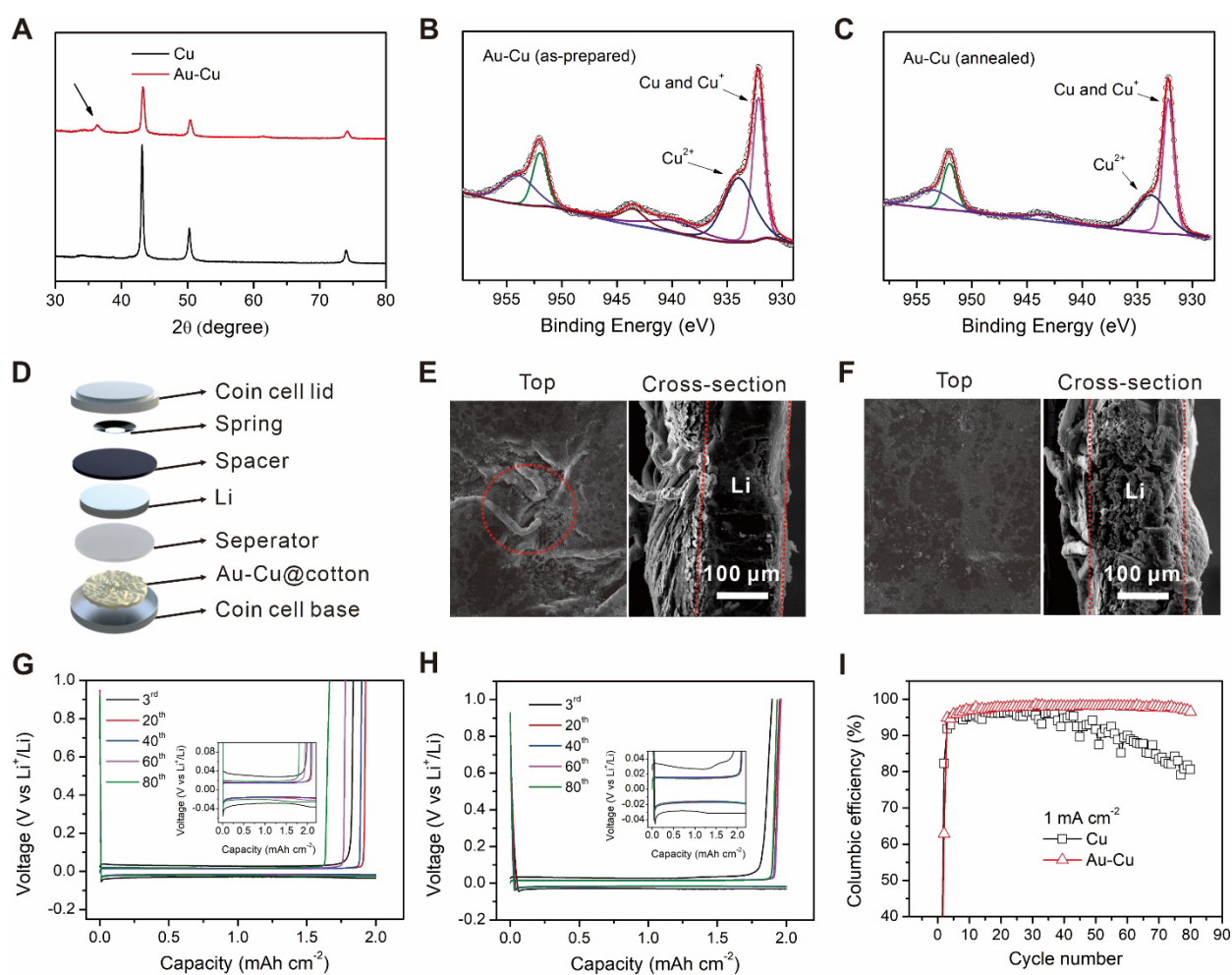


Figure 4. Metal-coated textiles for Li metal batteries. (A) XRD patterns of Cu and Au-Cu on cotton fabrics. The arrow indicates the (111) peak of Cu_2O . (B) and (C) XPS $\text{Cu } 2p$ detailed spectra of as-prepared Au-Cu and annealed Au-Cu, respectively. (D) Schematic illustration of a coin cell

with the Au-Cu@cotton current collector. (E) and (F) SEM images of Li-plated Cu@cotton and Au-Cu@cotton current collectors, respectively. The red dashed circle in (E) labels the area with poor Li coverage. The dashed lines in the cross-section images indicate the areas plated with Li. (G) and (H) The charge and discharge curves of coin cells with Cu@cotton and Au-Cu@cotton current collectors, respectively (enlarged plots are shown in insets). (I) Columbic efficiencies of coin cells based on Cu@cotton and Au-Cu@cotton current collectors during 80 charge and discharge cycles.

Conclusions

In summary, we have reported a facile and R2R-compatible solution process, namely r-PAMD, to deposit metals on multiple hydrophilic and hydrophobic textiles such as cotton, glass fiber, Kevlar, polyester, nylon, and carbon cloth. In comparison to all the existing technologies, r-PAMD significantly shortens the pretreatment process from tens of minutes or even hours to 3 min, which makes it very convenient and low-cost for metal deposition on textiles. Importantly, r-PAMD required no destructive pretreatment of the textiles that may lead to deterioration of the textile properties. The E-textiles showed a good conductivity, a high mechanical strength, and a high adhesion during repeated wash and abrasion tests. As a result, the performance of strain sensors and the electrodes for ECG sensing based on the r-PAMD method was very stable under 50 machine washes and 2,000 abrasion rubbings. For the Li metal battery applications, the galvanic displacement of Au on r-PAMD Cu was found effective for improving the performance of batteries, because the displacement reaction generates Li-affinitive Au and Cu₂O. These results indicated a

great potential of the r-PAMD approach to fabricating a wide range of E-textile materials and devices toward wearable electronics.

Supporting Information

The Supporting Information is available free of charge at XXXX.

- FTIR of the precursor mixture before and after UV irradiation, water contact angle on raw carbon cloth and polymer-modified carbon cloth, SEM top-view and EDX mapping of metal-coated textiles, photograph of a bundle of Cu-coated Kevlar yarns, tensile stress-strain curves of the raw Kevlar yarns and Cu-coated Kevlar yarns, the relative resistance change of the Cu-coated Kevlar knitted fabric during repeated stretch-compress test, photograph of a piece of cotton fabric coated with electroless-deposited Cu and electro-deposited Au, high resolution SEM images of Cu and Au-Cu coated cotton fibers, XPS survey of Cu, as-prepared Au-Cu, and annealed Au-Cu coated cotton fabrics, XPS patterns (Au 4f) of Au-Cu coated cotton fabrics before and after the thermal annealing process

Author Information

Corresponding Authors

Zijian Zheng - *Laboratory for Advanced Interfacial Materials and Devices, School of Fashion and Textiles, the Hong Kong Polytechnic University, Hong Kong, China; Research Institute for Intelligent Wearable Systems, The Hong Kong Polytechnic University, Hong Kong SAR, China; Department of Applied Biology and Chemical Technology, Faculty of Science, The Hong Kong*

Polytechnic University, Hong Kong SAR, China; Research Institute for Smart Energy, The Hong Kong Polytechnic University, Hong Kong SAR, China; Email: zijian.zheng@polyu.edu.hk

Authors

Yaokang Zhang - *Laboratory for Advanced Interfacial Materials and Devices, School of Fashion and Textiles, the Hong Kong Polytechnic University, Hong Kong, China*

Yufeng Luo - *Laboratory for Advanced Interfacial Materials and Devices, School of Fashion and Textiles, the Hong Kong Polytechnic University, Hong Kong, China*

Lei Wang - *Laboratory for Advanced Interfacial Materials and Devices, School of Fashion and Textiles, the Hong Kong Polytechnic University, Hong Kong, China*

Pui Fai Ng - *Laboratory for Advanced Interfacial Materials and Devices, School of Fashion and Textiles, the Hong Kong Polytechnic University, Hong Kong, China*

Hong Hu - *Laboratory for Advanced Interfacial Materials and Devices, School of Fashion and Textiles, the Hong Kong Polytechnic University, Hong Kong, China*

Fan Chen - *Laboratory for Advanced Interfacial Materials and Devices, School of Fashion and Textiles, the Hong Kong Polytechnic University, Hong Kong, China*

Qiyao Huang - *Laboratory for Advanced Interfacial Materials and Devices, School of Fashion and Textiles, the Hong Kong Polytechnic University, Hong Kong, China*

Author Contributions

Y.Z. and Y.L. contributed equally to this work. The study was conceived by Y.Z. and Z.J.Z. Y.Z., P.F.N., H.H., F.C., Q.H., and Z.J.Z. discussed the characterization of metal-coated textiles and sensors. Y.Z. and Y.L. fabricated and characterized the Li metal batteries. Y.Z., L.W., and Y.L. discussed the performance of Li metal batteries. Y.Z. and Z.J.Z. wrote the manuscript, and all authors contributed to the manuscript. Z.J.Z. approves the completed version.

Notes

The authors declare no competing financial interest.

Acknowledgements

This work is supported by the Hong Kong Polytechnic University (1-ZVT8, 1-YXA1), the Science and Technology Bureau of Huangpu District (202GH03), the Innovation and Technology Fund-Guangdong-Hong Kong Technology Cooperation Funding Scheme (ITF-TCFS, GHP/047/20GD).

References

- (1) Zhao, Z.; Huang, Q.; Yan, C.; Liu, Y.; Zeng, X.; Wei, X.; Hu, Y.; Zheng, Z. Machine-washable and Breathable Pressure Sensors Based on Triboelectric Nanogenerators Enabled by Textile Technologies. *Nano Energy* **2020**, *70*, 104528. DOI: <https://doi.org/10.1016/j.nanoen.2020.104528>.
- (2) Liu, Z.; Zheng, Y.; Jin, L.; Chen, K.; Zhai, H.; Huang, Q.; Chen, Z.; Yi, Y.; Umar, M.; Xu, L.; Li, G.; Song, Q.; Yue, P.; Li, Y.; Zheng, Z. Highly Breathable and Stretchable Strain Sensors with Insensitive

Response to Pressure and Bending. *Adv. Funct. Mater.* **2021**, *31*, 2007622. DOI: <https://doi.org/10.1002/adfm.202007622>.

(3) Zhen, H.; Li, K.; Chen, C.; Yu, Y.; Zheng, Z.; Ling, Q. Water-borne Foldable Polymer Solar Cells: One-step Transferring Free-standing Polymer Films onto Woven Fabric Electrodes. *J. Mater. Chem. A* **2017**, *5*, 782-788. DOI: 10.1039/C6TA08309A.

(4) Pullanchiyodan, A.; Manjakkal, L.; Dervin, S.; Shakthivel, D.; Dahiya, R. Metal Coated Conductive Fabrics with Graphite Electrodes and Biocompatible Gel Electrolyte for Wearable Supercapacitors. *Adv. Mater. Technol.* **2020**, *5*, 1901107. DOI: <https://doi.org/10.1002/admt.201901107>.

(5) Huang, Q.; Liu, L.; Wang, D.; Liu, J.; Huang, Z.; Zheng, Z. One-Step Electrospinning of Carbon Nanowebs on Metallic Textiles for High-Capacitance Supercapacitor Fabrics. *J. Mater. Chem. A* **2016**, *4*, 6802-6808. DOI: 10.1039/C5TA09309K.

(6) Yang, B.; Xiong, Y.; Ma, K.; Liu, S.; Tao, X. Recent Advances in Wearable Textile-based Triboelectric Generator Systems for Energy Harvesting from Human Motion. *EcoMat* **2020**, *2*, e12054. DOI: <https://doi.org/10.1002/eom2.12054>.

(7) Gao, Y.; Hu, H.; Chang, J.; Huang, Q.; Zhuang, Q.; Li, P.; Zheng, Z. Realizing High-Energy and Stable Wire-Type Batteries with Flexible Lithium–Metal Composite Yarns. *Adv. Energy Mater.* **2021**, *11*, 2101809. DOI: <https://doi.org/10.1002/aenm.202101809>.

(8) Chang, J.; Shang, J.; Sun, Y.; Ono, L. K.; Wang, D.; Ma, Z.; Huang, Q.; Chen, D.; Liu, G.; Cui, Y.; Qi, Y.; Zheng, Z. Flexible and Stable High-Energy Lithium-Sulfur Full Batteries with Only 100% Oversized Lithium. *Nat. Comm.* **2018**, *9*, 4480. DOI: 10.1038/s41467-018-06879-7.

(9) Kwon, S.; Kim, H.; Choi, S.; Jeong, E. G.; Kim, D.; Lee, S.; Lee, H. S.; Seo, Y. C.; Choi, K. C. Weavable and Highly Efficient Organic Light-Emitting Fibers for Wearable Electronics: A Scalable, Low-Temperature Process. *Nano Lett.* **2018**, *18*, 347-356. DOI: 10.1021/acs.nanolett.7b04204.

(10) Wang, D.; Zhang, Y.; Lu, X.; Ma, Z.; Xie, C.; Zheng, Z. Chemical Formation of Soft Metal Electrodes for Flexible and Wearable Electronics. *Chem. Soc. Rev.* **2018**, *47*, 4611-4641. DOI: 10.1039/C7CS00192D.

- (11) Yu, Y.; Zhang, Y.; Li, K.; Yan, C.; Zheng, Z. Bio-Inspired Chemical Fabrication of Stretchable Transparent Electrodes. *Small* **2015**, *11*, 3444-3449. DOI: <https://doi.org/10.1002/sml.201500529>.
- (12) Stoppa, M.; Chiolerio, A. Wearable Electronics and Smart Textiles: A Critical Review. *Sensors* **2014**, *14*, 11957-11992.
- (13) Fan, J. A.; Yeo, W.-H.; Su, Y.; Hattori, Y.; Lee, W.; Jung, S.-Y.; Zhang, Y.; Liu, Z.; Cheng, H.; Falgout, L.; Bajema, M.; Coleman, T.; Gregoire, D.; Larsen, R. J.; Huang, Y.; Rogers, J. A. Fractal Design Concepts for Stretchable Electronics. *Nat. Comm.* **2014**, *5*, 3266. DOI: 10.1038/ncomms4266.
- (14) Korzeniewska, E.; De Mey, G.; Pawlak, R.; Stempień, Z. Analysis of Resistance to Bending of Metal Electroconductive Layers Deposited on Textile Composite Substrates in PVD Process. *Sci. Rep.* **2020**, *10*, 8310. DOI: 10.1038/s41598-020-65316-2.
- (15) Ji, S.; Cho, G. Y.; Yu, W.; Su, P.-C.; Lee, M. H.; Cha, S. W. Plasma-Enhanced Atomic Layer Deposition of Nanoscale Yttria-Stabilized Zirconia Electrolyte for Solid Oxide Fuel Cells with Porous Substrate. *ACS Appl. Mater. Interfaces* **2015**, *7*, 2998-3002. DOI: 10.1021/am508710s.
- (16) Lee, H. M.; Choi, S. Y.; Jung, A.; Ko, S. H. Highly Conductive Aluminum Textile and Paper for Flexible and Wearable Electronics. *Angew. Chem.* **2013**, *125*, 7872-7877.
- (17) Wang, Y.-F.; Wang, H.-T.; Yang, S.-Y.; Yue, Y.; Bian, S.-W. Hierarchical NiCo₂S₄@Nickel-Cobalt Layered Double Hydroxide Nanotube Arrays on Metallic Cotton Yarns for Flexible Supercapacitors. *ACS Appl. Mater. Interfaces* **2019**, *11*, 30384-30390. DOI: 10.1021/acsami.9b06317.
- (18) Lu, X.; Shang, W.; Chen, G.; Wang, H.; Tan, P.; Deng, X.; Song, H.; Xu, Z.; Huang, J.; Zhou, X. Environmentally Stable, Highly Conductive, and Mechanically Robust Metallized Textiles. *ACS Appl. Electron. Mater.* **2021**, *3*, 1477-1488. DOI: 10.1021/acsaelm.1c00088.
- (19) Bae, S.; Kim, H.; Lee, Y.; Xu, X.; Park, J.-S.; Zheng, Y.; Balakrishnan, J.; Lei, T.; Ri Kim, H.; Song, Y. I.; Kim, Y.-J.; Kim, K. S.; Özyilmaz, B.; Ahn, J.-H.; Hong, B. H.; Iijima, S. Roll-To-Roll Production of 30-Inch Graphene Films for Transparent Electrodes. *Nat. Nanotech.* **2010**, *5*, 574-578. DOI: 10.1038/nnano.2010.132.

- (20) Søndergaard, R. R.; Hösel, M.; Krebs, F. C. Roll-to-Roll Fabrication of Large Area Functional Organic Materials. *J. Polym. Sci., Part B: Polym. Phys.* **2013**, *51*, 16-34. DOI: <https://doi.org/10.1002/polb.23192>.
- (21) Gregory, R. V.; Kimbrell, W. C.; Kuhn, H. H. Conductive Textiles. *Synth. Met.* **1989**, *28*, 823-835. DOI: [https://doi.org/10.1016/0379-6779\(89\)90610-3](https://doi.org/10.1016/0379-6779(89)90610-3).
- (22) Liu, X.; Chang, H.; Li, Y.; Huck, W. T. S.; Zheng, Z. Polyelectrolyte-Bridged Metal/Cotton Hierarchical Structures for Highly Durable Conductive Yarns. *ACS Appl. Mater. Interfaces* **2010**, *2*, 529-535. DOI: 10.1021/am900744n.
- (23) Liu, X.; Zhou, X.; Li, Y.; Zheng, Z. Surface-Grafted Polymer-Assisted Electroless Deposition of Metals for Flexible and Stretchable Electronics. *Chem. Asian J.* **2012**, *7*, 862-870. DOI: <https://doi.org/10.1002/asia.201100946>.
- (24) Grell, M.; Dincer, C.; Le, T.; Lauri, A.; Nunez Bajo, E.; Kasimatis, M.; Barandun, G.; Maier, S. A.; Cass, A. E. G.; Güder, F. Autocatalytic Metallization of Fabrics Using Si Ink, for Biosensors, Batteries and Energy Harvesting. *Adv. Funct. Mater.* **2019**, *29*, 1804798. DOI: <https://doi.org/10.1002/adfm.201804798>.
- (25) Wei, X.; Roper, D. K. Tin Sensitization for Electroless Plating Review. *J. Electrochem. Soc.* **2014**, *161*, D235-D242. DOI: 10.1149/2.047405jes.
- (26) Lee, S.; Wajahat, M.; Kim, J. H.; Pyo, J.; Chang, W. S.; Cho, S. H.; Kim, J. T.; Seol, S. K. Electroless Deposition-Assisted 3D Printing of Micro Circuitries for Structural Electronics. *ACS Appl. Mater. Interfaces* **2019**, *11*, 7123-7130. DOI: 10.1021/acsami.8b18199.
- (27) Frunza, L.; Preda, N.; Matei, E.; Frunza, S.; Ganea, C. P.; Vlaicu, A. M.; Diamandescu, L.; Dorogan, A. Synthetic Fabrics Coated with Zinc Oxide Nanoparticles by Electroless Deposition: Structural Characterization and Wetting Properties. *J. Polym. Sci., Part B: Polym. Phys.* **2013**, *51*, 1427-1437. DOI: <https://doi.org/10.1002/polb.23346>.
- (28) Zille, A.; Fernandes, M. M.; Francesko, A.; Tzanov, T.; Fernandes, M.; Oliveira, F. R.; Almeida, L.; Amorim, T.; Carneiro, N.; Esteves, M. F.; Souto, A. P. Size and Aging Effects on Antimicrobial Efficiency of Silver Nanoparticles Coated on Polyamide Fabrics Activated by Atmospheric DBD Plasma. *ACS Appl. Mater. Interfaces* **2015**, *7*, 13731-13744. DOI: 10.1021/acsami.5b04340.

- (29) Ratautas, K.; Andrulevičius, M.; Jagminienė, A.; Stankevičienė, I.; Norkus, E.; Račiukaitis, G. Laser-assisted Selective Copper Deposition on Commercial PA6 by Catalytic Electroless Plating – Process and Activation Mechanism. *Appl. Surf. Sci.* **2019**, *470*, 405-410. DOI: <https://doi.org/10.1016/j.apsusc.2018.11.091>.
- (30) Tamai, T.; Watanabe, M.; Kobayashi, Y.; Kobata, J.; Nakahara, Y.; Yajima, S. Surface Modification of Polyethylene Naphthalate Substrates by Ultraviolet Light-irradiation and Assembling Multilayers and Their Application in Electroless Deposition: The Chemical and Physical Properties of the Stratified Structure. *Colloids Surf. Physicochem. Eng. Aspects* **2019**, *575*, 230-236. DOI: <https://doi.org/10.1016/j.colsurfa.2019.05.017>.
- (31) Zhao, H.; Hou, L.; Bi, S.; Lu, Y. Enhanced X-Band Electromagnetic-Interference Shielding Performance of Layer-Structured Fabric-Supported Polyaniline/Cobalt–Nickel Coatings. *ACS Appl. Mater. Interfaces* **2017**, *9*, 33059-33070. DOI: [10.1021/acsami.7b07941](https://doi.org/10.1021/acsami.7b07941).
- (32) Han, E. G.; Kim, E. A.; Oh, K. W. Electromagnetic Interference Shielding Effectiveness of Electroless Cu-plated PET Fabrics. *Synth. Met.* **2001**, *123*, 469-476. DOI: [https://doi.org/10.1016/S0379-6779\(01\)00332-0](https://doi.org/10.1016/S0379-6779(01)00332-0).
- (33) Guo, R. H.; Jiang, S. X.; Zheng, Y. D.; Lan, J. W. Electroless Nickel Deposition of A Palladium-Activated Self-Assembled Monolayer on Polyester Fabric. *J. Appl. Polym. Sci.* **2013**, *127*, 4186-4193. DOI: <https://doi.org/10.1002/app.36799>.
- (34) Yu, Y.; Yan, C.; Zheng, Z. Polymer-Assisted Metal Deposition (PAMD): A Full-Solution Strategy for Flexible, Stretchable, Compressible, and Wearable Metal Conductors. *Adv. Mater.* **2014**, *26*, 5508-5516. DOI: <https://doi.org/10.1002/adma.201305558>.
- (35) Li, P.; Zhang, Y.; Zheng, Z. Polymer-Assisted Metal Deposition (PAMD) for Flexible and Wearable Electronics: Principle, Materials, Printing, and Devices. *Adv. Mater.* **2019**, *31*, 1902987. DOI: <https://doi.org/10.1002/adma.201902987>.

- (36) Guo, R.; Li, H.; Wang, H.; Zhao, X.; Yu, H.; Ye, Q. Polydimethylsiloxane-Assisted Catalytic Printing for Highly Conductive, Adhesive, and Precise Metal Patterns Enabled on Paper and Textiles. *ACS Appl. Mater. Interfaces* **2021**, *13*, 56597-56606. DOI: 10.1021/acsami.1c18065.
- (37) Azzaroni, O.; Moya, S. E.; Brown, A. A.; Zheng, Z.; Donath, E.; Huck, W. T. S. Polyelectrolyte Brushes as Ink Nanoreservoirs for Microcontact Printing of Ionic Species with Poly(dimethyl siloxane) Stamps. *Adv. Funct. Mater.* **2006**, *16*, 1037-1042. DOI: <https://doi.org/10.1002/adfm.200500702>.
- (38) Wang, X.; Yan, C.; Hu, H.; Zhou, X.; Guo, R.; Liu, X.; Xie, Z.; Huang, Z.; Zheng, Z. Aqueous and Air-Compatible Fabrication of High-Performance Conductive Textiles. *Chem. Asian J.* **2014**, *9*, 2170-2177. DOI: <https://doi.org/10.1002/asia.201402230>.
- (39) Guo, R.; Yu, Y.; Xie, Z.; Liu, X.; Zhou, X.; Gao, Y.; Liu, Z.; Zhou, F.; Yang, Y.; Zheng, Z. Matrix-Assisted Catalytic Printing for the Fabrication of Multiscale, Flexible, Foldable, and Stretchable Metal Conductors. *Adv. Mater.* **2013**, *25*, 3343-3350. DOI: <https://doi.org/10.1002/adma.201301184>.
- (40) Allahyarzadeh, V.; Montazer, M.; Nejad, N. H.; Samadi, N. In Situ Synthesis of Nano Silver on Polyester Using NaOH/Nano TiO₂. *J. Appl. Polym. Sci.* **2013**, *129*, 892-900. DOI: <https://doi.org/10.1002/app.38907>.
- (41) Zeronian, S. H.; Collins, M. J. Surface Modification of Polyester by Alkaline Treatments. *Text. Prog.* **1989**, *20*, 1-26.
- (42) Wang, X. C.; Zheng, H. Y.; Lim, G. C. Laser Induced Copper Electroless Plating on Polyimide with Q-switch Nd:YAG Laser. *Appl. Surf. Sci.* **2002**, *200*, 165-171. DOI: [https://doi.org/10.1016/S0169-4332\(02\)00850-4](https://doi.org/10.1016/S0169-4332(02)00850-4).
- (43) Yu, D.; Kang, G.; Tian, W.; Lin, L.; Wang, W. Preparation of Conductive Silk Fabric with Antibacterial Properties by Electroless Silver Plating. *Appl. Surf. Sci.* **2015**, *357*, 1157-1162. DOI: <https://doi.org/10.1016/j.apsusc.2015.09.074>.
- (44) Long, J.-J.; Wang, H.-W.; Lu, T.-Q.; Tang, R.-C.; Zhu, Y.-w. Application of Low-Pressure Plasma Pretreatment in Silk Fabric Degumming Process. *Plasma Chem. Plasma Process.* **2008**, *28*, 701-713. DOI: 10.1007/s11090-008-9153-z.

- (45) Jayabal, S.; Sathiyamurthy, S.; Loganathan, K. T.; Kalyanasundaram, S. Effect of Soaking Time and Concentration of NaOH Solution On Mechanical Properties of Coir–polyester Composites. *Bull. Mater. Sci.* **2012**, *35*, 567-574. DOI: 10.1007/s12034-012-0334-2.
- (46) Lund, A.; Darabi, S.; Hultmark, S.; Ryan, J. D.; Andersson, B.; Ström, A.; Müller, C. Roll-to-Roll Dyed Conducting Silk Yarns: A Versatile Material for E-Textile Devices. *Adv. Mater. Technol.* **2018**, *3*, 1800251. DOI: <https://doi.org/10.1002/admt.201800251>.
- (47) Taghavi Pourian Azar, G.; Fox, D.; Fedutik, Y.; Krishnan, L.; Cobley, A. J. Functionalised Copper Nanoparticle Catalysts for Electroless Copper Plating on Textiles. *Surf. Coat. Technol.* **2020**, *396*, 125971. DOI: <https://doi.org/10.1016/j.surfcoat.2020.125971>.
- (48) Pu, X.; Liu, M.; Li, L.; Han, S.; Li, X.; Jiang, C.; Du, C.; Luo, J.; Hu, W.; Wang, Z. L. Wearable Textile-Based In-Plane Microsupercapacitors. *Adv. Energy Mater.* **2016**, *6*, 1601254. DOI: <https://doi.org/10.1002/aenm.201601254>.
- (49) Sano, M.; Tahara, Y.; Chen, C.-Y.; Chang, T.-F. M.; Hashimoto, T.; Kurosu, H.; Sato, T.; Sone, M. Application of Supercritical Carbon Dioxide in Catalyzation and Ni-P Electroless Plating of Nylon 6,6 Textile. *Surf. Coat. Technol.* **2016**, *302*, 336-343. DOI: <https://doi.org/10.1016/j.surfcoat.2016.06.037>.
- (50) Wang, D.; Sun, J.; Xue, Q.; Li, Q.; Guo, Y.; Zhao, Y.; Chen, Z.; Huang, Z.; Yang, Q.; Liang, G.; Dong, B.; Zhi, C. A Universal Method Towards Conductive Textile for Flexible Batteries with Superior Softness. *Energy Storage Mater.* **2021**, *36*, 272-278. DOI: <https://doi.org/10.1016/j.ensm.2021.01.001>.
- (51) Zhu, C.; Li, R.; Chen, X.; Chalmers, E.; Liu, X.; Wang, Y.; Xu, B. B.; Liu, X. Ultraelastic Yarns from Curcumin-Assisted ELD toward Wearable Human–Machine Interface Textiles. *Adv. Sci.* **2020**, *7*, 2002009. DOI: <https://doi.org/10.1002/advs.202002009>.
- (52) Cai, L.; Song, A. Y.; Wu, P.; Hsu, P.-C.; Peng, Y.; Chen, J.; Liu, C.; Catrysse, P. B.; Liu, Y.; Yang, A.; Zhou, C.; Zhou, C.; Fan, S.; Cui, Y. Warming Up Human Body by Nanoporous Metallized Polyethylene Textile. *Nat. Comm.* **2017**, *8*, 496. DOI: 10.1038/s41467-017-00614-4.
- (53) Yu, Y.; Xiao, X.; Zhang, Y.; Li, K.; Yan, C.; Wei, X.; Chen, L.; Zhen, H.; Zhou, H.; Zhang, S.; Zheng, Z. Photoreactive and Metal-Platable Copolymer Inks for High-Throughput, Room-Temperature Printing of

Flexible Metal Electrodes for Thin-Film Electronics. *Adv. Mater.* **2016**, *28*, 4926-4934. DOI: <https://doi.org/10.1002/adma.201505119>.

(54) Friis, J. E.; Brøns, K.; Salmi, Z.; Shimizu, K.; Subbiahdoss, G.; Holm, A. H.; Santos, O.; Pedersen, S. U.; Meyer, R. L.; Daasbjerg, K.; Iruthayaraj, J. Hydrophilic Polymer Brush Layers on Stainless Steel Using Multilayered ATRP Initiator Layer. *ACS Appl. Mater. Interfaces* **2016**, *8*, 30616-30627. DOI: 10.1021/acsami.6b10466.

(55) Zhao, Z.; Yan, C.; Liu, Z.; Fu, X.; Peng, L.-M.; Hu, Y.; Zheng, Z. Machine-Washable Textile Triboelectric Nanogenerators for Effective Human Respiratory Monitoring through Loom Weaving of Metallic Yarns. *Adv. Mater.* **2016**, *28*, 10267-10274. DOI: <https://doi.org/10.1002/adma.201603679>.

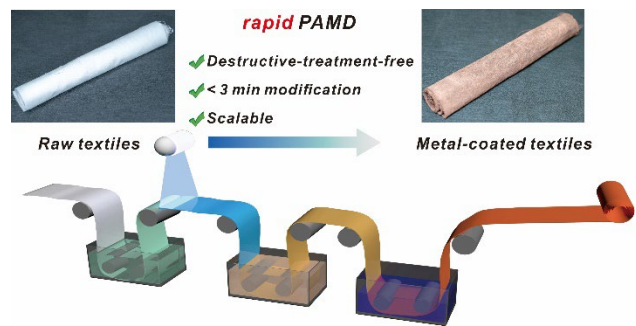
(56) Liang, Y.; Chen, Y.; Ke, X.; Zhang, Z.; Wu, W.; Lin, G.; Zhou, Z.; Shi, Z. Coupling of Triporosity and Strong Au–Li Interaction to Enable Dendrite-free Lithium Plating/Stripping for Long-life Lithium Metal Anodes. *J. Mater. Chem. A* **2020**, *8*, 18094-18105. DOI: 10.1039/D0TA04768F.

(57) Chang, J.; Hu, H.; Shang, J.; Fang, R.; Shou, D.; Xie, C.; Gao, Y.; Yang, Y.; Zhuang, Q. N.; Lu, X.; Zhang, Y. K.; Li, F.; Zheng, Z. Rational Design of Li-Wicking Hosts for Ultrafast Fabrication of Flexible and Stable Lithium Metal Anodes. *Small* **2022**, *18*, 2105308. DOI: <https://doi.org/10.1002/sml.202105308>.

(58) Zhang, Y.; Guo, X.; Huang, J.; Ren, Z.; Hu, H.; Li, P.; Lu, X.; Wu, Z.; Xiao, T.; Zhu, Y.; Li, G.; Zheng, Z. Solution Process Formation of High Performance, Stable Nanostructured Transparent Metal Electrodes via Displacement-Diffusion-Etch Process. *npj Flex. Electron.* **2022**, *6*, 4. DOI: 10.1038/s41528-022-00134-2.

(59) Lee, S. Y.; Mettlach, N.; Nguyen, N.; Sun, Y. M.; White, J. M. Copper Oxide Reduction Through Vacuum Annealing. *Appl. Surf. Sci.* **2003**, *206*, 102-109. DOI: [https://doi.org/10.1016/S0169-4332\(02\)01239-4](https://doi.org/10.1016/S0169-4332(02)01239-4).

(60) Qi, Z.; Tang, J.; Misra, S.; Fan, C.; Lu, P.; Jian, J.; He, Z.; Pol, V. G.; Zhang, X.; Wang, H. Enhancing Electrochemical Performance of Thin Film Lithium Ion Battery via Introducing Tilted Metal Nanopillars as Effective Current Collectors. *Nano Energy* **2020**, *69*, 104381. DOI: <https://doi.org/10.1016/j.nanoen.2019.104381>.



For Table of Contents Only